P3.3

LONG-TERM VALIDATION AND VARIABILITY OF THE SHORTWAVE AND LONGWAVE RADIATION DATA OF THE GEWEX SURFACE RADIATION BUDGET (SRB) PROJECT

Taiping Zhang[1*], Paul W. Stackhouse Jr.[2], Shashi K. Gupta[1], Stephan J. Cox[1], Colleen Mikovitz[1], Laura M. Hinkelman[3]
[1]AS & M/NASA Langley Research Center, Hampton, Virginia
[2]NASA Langley Research Center, Hampton, Virginia
[3]National Institute of Aerospace, NASA Langley Research Center, Hampton, Virginia

1 INTRODUCTION

The Surface Radiation Budget (SRB) project is a significant component of the Global Energy and Water Cycle Experiment (GEWEX) (*e.g.*, Pinker *et al.*, 2003; Randall *et al.*, 2003). Targeted at its objective, SRB has produced and archived a global 21.5 year (July 1983-December 2004) climatology of, among a long list of other related variables, shortwave/longwave (SW/LW) downward/upward radiation fluxes at the Earth's surface using the algorithm of the NASA World Climate Research Programme (WCRP) (Versions 2.5 and 2.6) which include the Global Earth Observing System (GEOS) Version 4.0.3 meteorological information in its inputs (Suarez, 2005). (The earlier versions of these data sets have been studied from different perspectives. (*e.g.*, Gupta *et al.*, 1999; Zhang *et al.*, 2003; Zhang *et al.*, 2004; Pinker, Zhang and Dutton, 2005).

The uncertainties in the atmospheric information and imperfect algorithms in radiation transfer models make the satellite-derived surface information uncertain. Therefore, ground-based observations are indispensable for corroboration and ultimate validation of the surface information derived from satellite-observations. At the same time, surface observations can be used to train radiation transfer models. Additionally, the surface observations are more reliable for detecting long-term trend related to climate change.

For this reason, the GEWEX program has a Baseline Surface Radiation Network (BSRN) designed to specialize in ground-based observations. In this study we use 2849 site-months of BSRN data representing 35 ground stations.

*Corresponding author address: Taiping Zhang, AS & M/NASA Langley Research Center, Mail Stop 936, Hampton, VA 23681-2199

In addition, we use the World Radiation Data Centre (WRDC) and Global Energy Balance Archive (GEBA) data. The WRDC data used here include daily means of shortwave downward fluxes from 474 sites of the World Radiation Data Centre (WRDC) depository. The GEBA data include monthly means of shortwave downward fluxes from 797 sites and longwave from 20 sites.

In this investigation, we make systematic SRB-BSRN, SRB-WRDC and SRB-GEBA comparisons for both shortwave and longwave daily and monthly mean radiation fluxes at the Earth's surface.

We first have an overview of all the comparable pairs of data in scatter or scatter density plots. Then we show the time series of the SRB data at grids in which there are ground sites where long-term records of data are available for comparison. An overall very good agreement between the SRB data and ground observations is found.

To see the variablity of the SRB data during the 21.5 years, we computed the global mean and its linear trend. No appreciable trend is detected at the 5% level.

The empirical orthogonal functions (EOF) of the SRB deseasonalized shortwave downward flux are computed over the Pacific region, and the first EOF coefficient is found to be correlated with the ENSO Index at a high value of coefficient of 0.7083.

2 Data

The satellite data is the SRB data, and the ground-based data are from the BSRN, the WRDC and the GEBA databases.

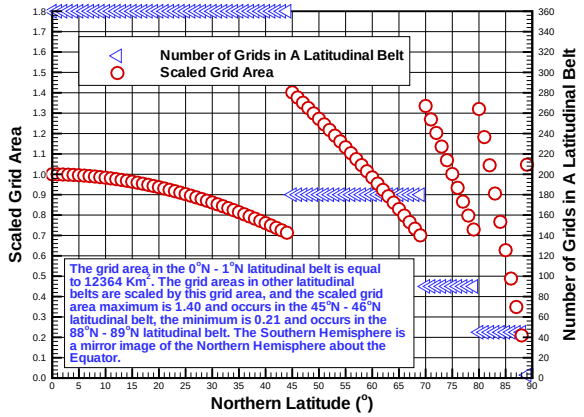

Figure 1: Scaled grid areas in each 1°-latitudinal belt. The globe is first divided into 180 1°-latitudinal belts. In Northern Hemisphere, from 0°N to 45°N, each belt has 360 grids; from 45°N to 70°N, each belt has 180 grids; from 70°N to 80°N, each belt has 90 grids; from 80°N to 89°N, each belt has 45 grids; from 89°N to 90°N, the belt has 3 grids. The Southern Hemisphere is a mirror image of the Northern Hemisphere about the Equator.

2.1 The SRB Data

The SRB data are output of models designed for the SRB project, and the data sets are presented for a network of 44,016 grids of nearly equal area as shown in Figure 1. The Earth's surface is first divided into 1° latitudinal belts, and each such belt is then divided into grids of equal area, the number of grids depending on the latitude. In the tropical zone, the grids are $1^\circ \times 1^\circ$ and, the northernmost and southernmost belts are divided into $1^\circ \times 120^\circ$ grids.

2.2 The BSRN Data

We use the BSRN archived data worth 2849 site-months, representing 35 ground stations ranging from the northernmost one at Ny Ålesund in Spitsbergen (78.93° N, 11.95° E) to the southernmost one at South Pole (90° S), covering the time period from January 1992 to August 2004. The observed variables used in the current study are shortwave and longwave downward fluxes at the Earth's surface. The BSRN observations are made at 1-, 2, 3- or 5-minute intervals. More information about BSRN can be found in Ohmura *et al.* (1998); Philipona *et al.* (1998); McArthur, 1998; Wild *et al.* (2005). Figure 2 shows the locations of the 35 BSRN sites.

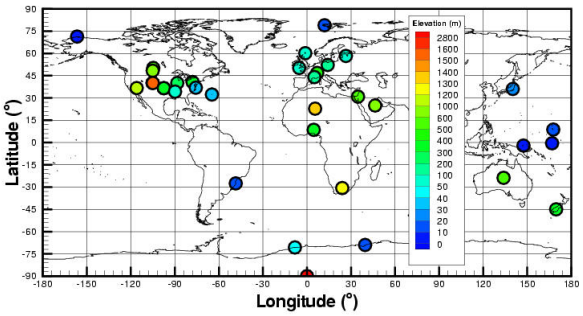

Figure 2: Baseline Surface Radiation Network (BSRN) sites with data.

The data are first processed to generate 3-hourly, 3-hourly-monthly, daily and monthly means so that they can be compared with their BSRN counterparts on the same time scales. Note that the SRB 3-hourly data represent instantaneous snapshots of the Earth at UTC 00:00, 03:00, 06:00, ..., 21:00 of averages over grids of about 11,588 Km^2, and these hours are called "time stamps". The BSRN 3-hourly means, on the other hand, are averages of all valid values observed at 1-, 2-, 3- or 5-minute intervals during 3-hour periods centered on the said "time stamps", and these averages represent single points on the ground. Contrary to the intuition, this approach actually makes the SRB 3-hourly data and corresponding BSRN 3-hourly means more comparable, as shall be made clearer later.

2.3 The WRDC Data

The World Radiation Data Centre (WRDC), established in accordance with Resolution 31 of WMO Executive Committee XVIII in 1964, is a central depository of solar radiation data collected over 1000 ground sites over the world. In this study, we use a subset of the WRDC data which includes daily mean shortwave downward flux from 474 sites throughout the world spanning the years 1983-1993. Out of these sites, 55 have continuous records, and the records at other sites are sporadic at various extent. Monthly means are computed whenever it is possible. Figure 3 shows the 474 WRDC sites.

2.4 The GEBA Data

The Global Energy Balance Archive (GEBA) is Project A7, Water (WMO/ICSU), of the World Climate Programme. In this study, we use the monthly

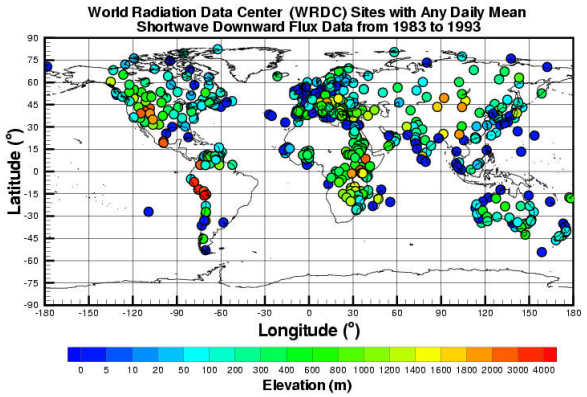

Figure 3: World Radiation Data Center (WRDC) sites with any data from 1983 to 1993.

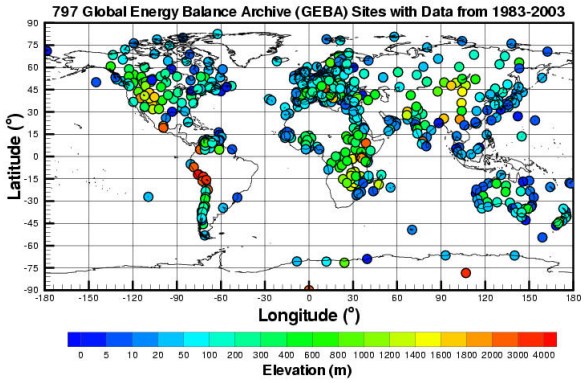

Figure 4: 797 Global Energy Balance Archive sites with data from 1983 to 2003.

means of shortwave downward fluxes from 797 GEBA sites and longwave from 20 GEBA sites. Figure 4 shows the shortwave GEBA sites.

3 The Comparison

Before we look at those ground sites with long-time records, we first have an overview of all available BSRN data points paired with their SRB counterparts in plots of scatters or scatter density, which include all sporadic yet valid data points.

3.1 An Overall View

Figure 5 shows the scatter density plot of *daily* mean SRB Version 2.6 shortwave downward fluxes versus their BSRN counterparts for the years 1992-2004. The 35 BSRN sites represented are shown in Figure 2. The reason that a *scatter density* plot is chosen over a *density* plot is that significant overlapping occurs in a plot of the latter kind due to the large number of data points. The color of a grid indicates the *relative* count of the data points in the grid which is the *absolute* count of the data points divided by the total, *i.e.*, N.

Figure 6 is the same as Figure 5 except it is the *monthly* mean and *scatters* in place of *scatter density* are plotted.

Figures 7 and 8 are the *longwave* counterparts of Figures 5 and 6.

Figures 9 and 10 are the same as Figures 5 and 6 except the ground-based observations are from the WRDC database. Note the large number of data points, $N = 1640247$, representing 655 different WRDC ground sites from 1983-1993 (Figure 3, in the daily means and the concentration of high values of density along the white line, the ideal situation. The derived monthly means, representing 474 ground-sites, still have a number of data points large enough to justify a scatter density plots.

The GEBA data are available only in *monthly* means. Figure 11 shows the monthly mean GEBA shortwave downward fluxes versus their SRB counterparts for the years 1983-2003. Both the numbers of GEBA ground sites and data points are larger than that of WRDC data. The 82,977 data points represent 797 ground sites as shown in Figure 4.

Only 19 of the GEBA sites have 1013 available monthly mean longwave downward flux data points which are shown in Figure 12 along with their SRB counterparts.

Generally speaking, the updated satellite-derived SRB data are in very good agreement with ground observations. In terms of the $Bias$ absolute value and RMS, the longwave data show much better agreement than the shortwave data for understandable reasons, and of the shortwave data, the GEBA data, with the largest numbers of ground sites and data points of all the three sets of ground-based data, show the best agreement with the SRB data.

3.2 Time-Series of Monthly Means

Fortunately, all the three sets of ground-based data have sites with considerably long records of observations.

Figures 13, 14 and 15 show the time series of monthly means of shortwave downward fluxes at BSRN sites NYA (Ny Ålesund, Spitzbergen), KWA (Kwajelein, Marshall Islands) and SPO (South Pole) for the years 1992-2003 along with their SRB counterparts.

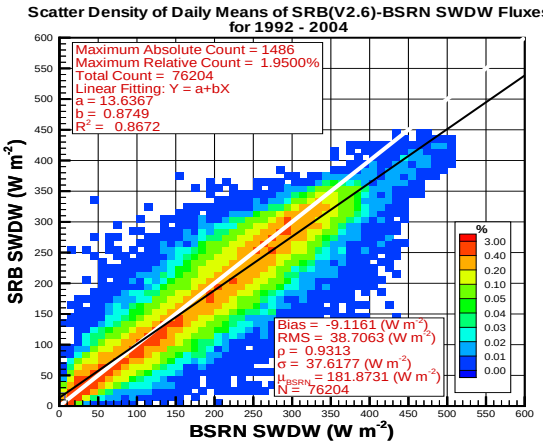

Figure 5: Scatter density of SRB(V2.6)-BSRN shortwave downward flux daily comparison.The white line represents the points where BSRN values are equal to their SRB counterparts, and the black line is the result of linear regression. R^2 is the coefficient of multiple determination; $Bias$ is the average of the SRB-BSRN difference, and RMS is the root mean square of the same difference; ρ is the SRB-BSRN correlation coefficient; σ is the standard deviation of the SRB-BSRN difference; μ_{BSRN} is the average of all BSRN data points; N is the total number of data points in the plot. The same nomenclature is used throughout the paper.

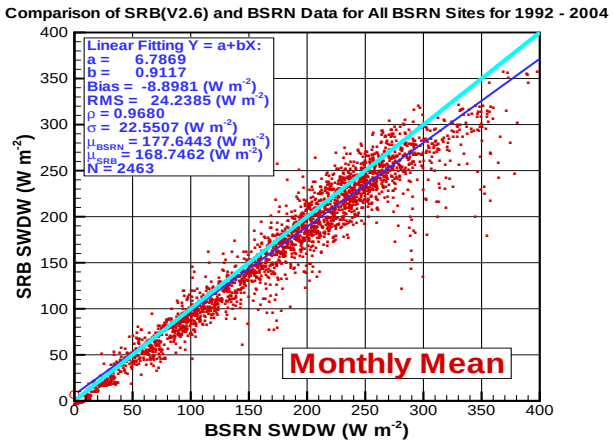

Figure 6: SRB(V2.6)-BSRN shortwave downward flux monthly mean comparisons.

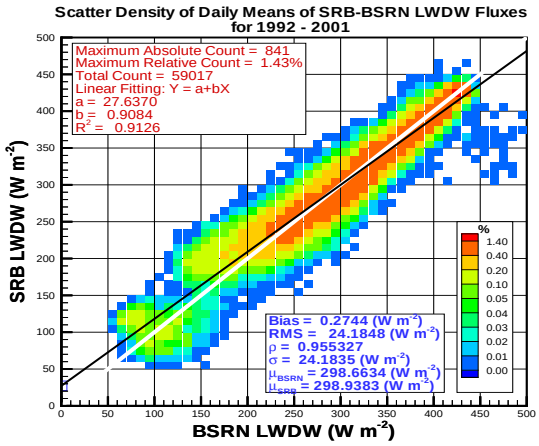

Figure 7: Scatter density of SRB(V2.5)-BSRN longwave downward flux daily mean comparison.

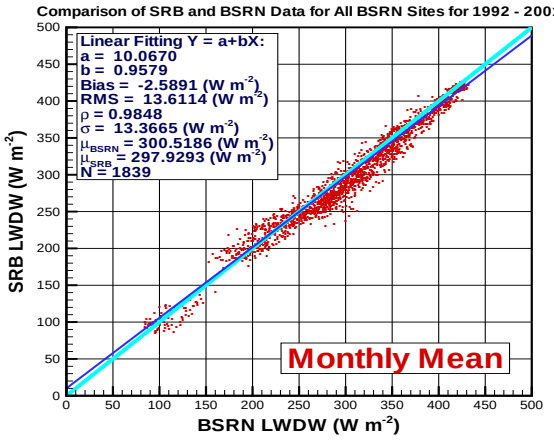

Figure 8: SRB(V2.5)-BSRN longwave downward flux monthly mean comparison.

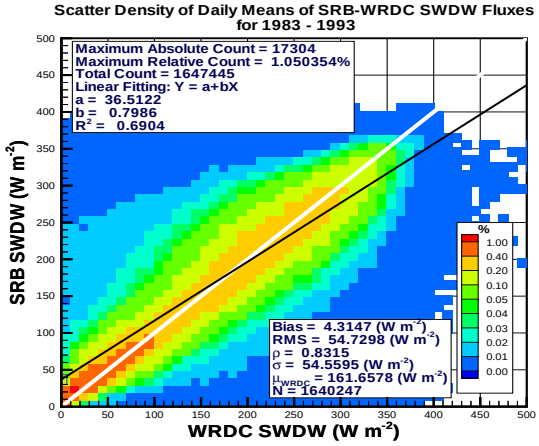

Figure 9: Scatter density of SRB(V2.5)-WRDC shortwave downward flux daily mean comparison.

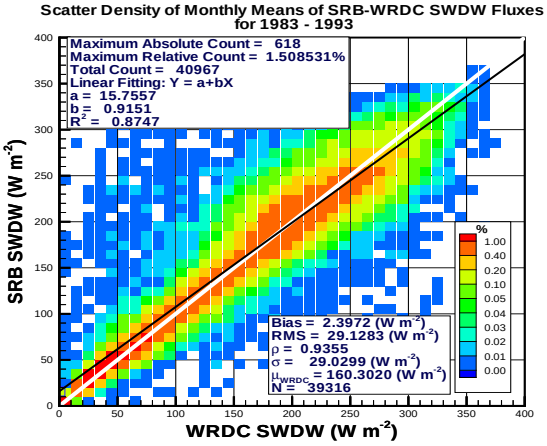

Figure 10: Scatter density of SRB(V2.5)-WRDC shortwave downward flux monthly mean comparison.

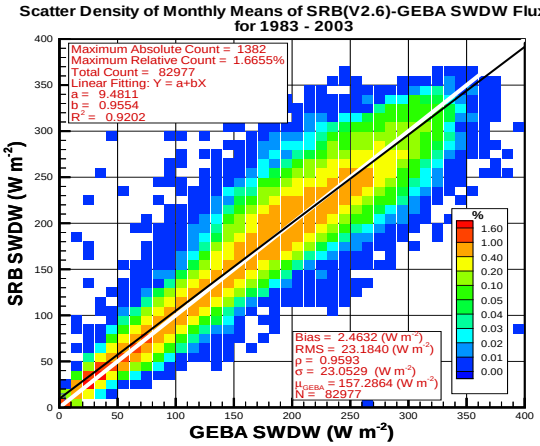

Figure 11: Scatter density of SRB(V2.6)-GEBA shortwave downward flux monthly mean comparison.

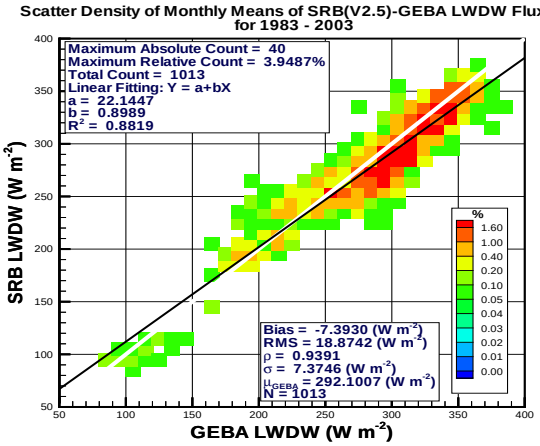

Figure 12: Scatter density of SRB(V2.5)-GEBA longwave downward flux monthly mean comparison.

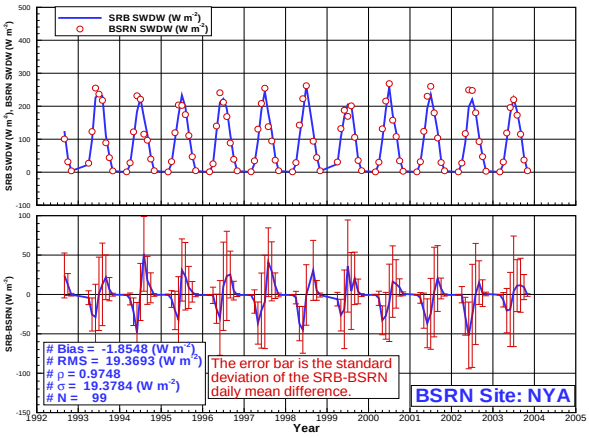

Figure 13: Time series of monthly means of SRB(V2.6) and BSRN shortwave downward fluxes and difference thereof at BSRN site NYA (Ny Ålesund, Spitzbergen; 78.93°N, 11.95°E).

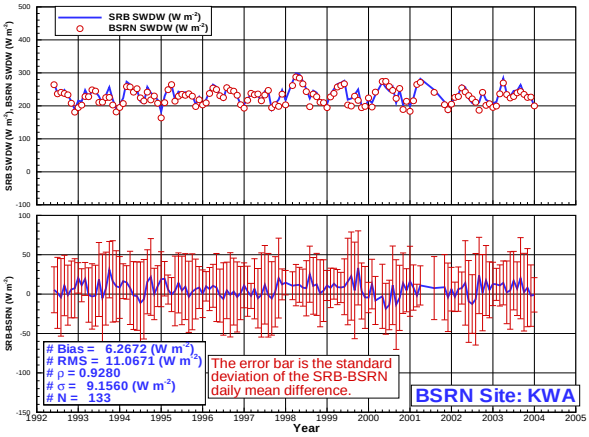

Figure 14: Time series of monthly means of SRB(V2.6) and BSRN shortwave downward fluxes and difference thereof at BSRN site KWA (Kwajalein, Marshall Islands; 8.72°N, 167.73°E).

Figures 16, 17 and 18 show the longwave counterparts of the above three BSRN sites.

Eight of the 35 BSRN sites have continuous records at the same time span.

Figures 19, 20, 21 and 22 show the time series of WRDC monthly mean shortwave downward fluxes for the years 1983-1993 at WRDC sites 0626 (Wrangel Island, Russia), 0350 (Klote, Switzerland), 0857 (Narok, Kenya), and 0953 (Bulawayo, Zimbabwe) along with their SRB counterparts.

Out of the 655 WRDC sites represented in this study, 55 have continuous records over the same time span.

Figures 23, 24, 25 and 26 show the time series of the GEBA monthly mean shortwave downward fluxes for the years 1983-2003 at GEBA sites 1412

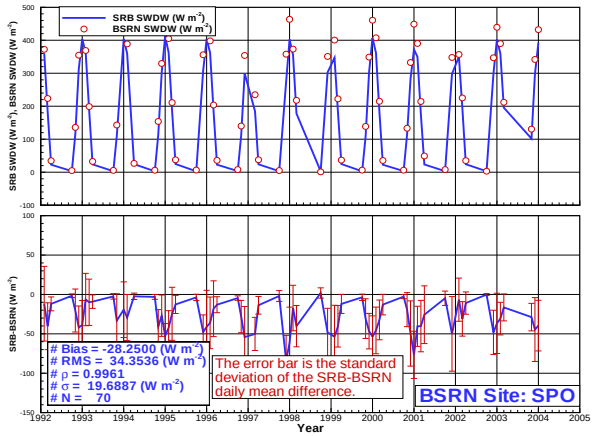

Figure 15: Time series of monthly means of SRB(V2.6) and BSRN shortwave downward fluxes and difference thereof at BSRN site SPO (South Pole; 90.00°S, 0.00°E).

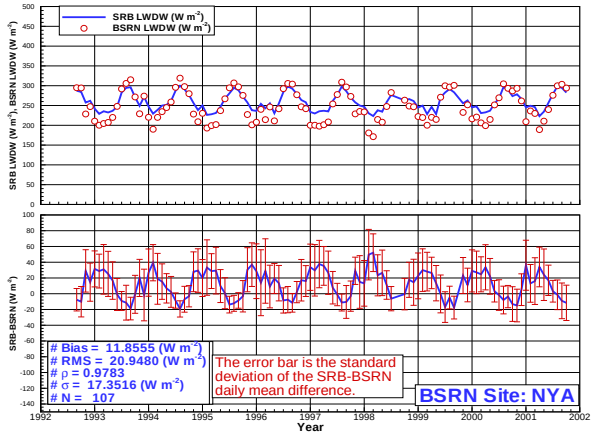

Figure 16: Time series of monthly means of SRB(V2.5) and BSRN longwave downward fluxes and difference thereof at BSRN site NYA (Ny Ålesund, Spitzbergen; 78.93°N, 11.95°E).

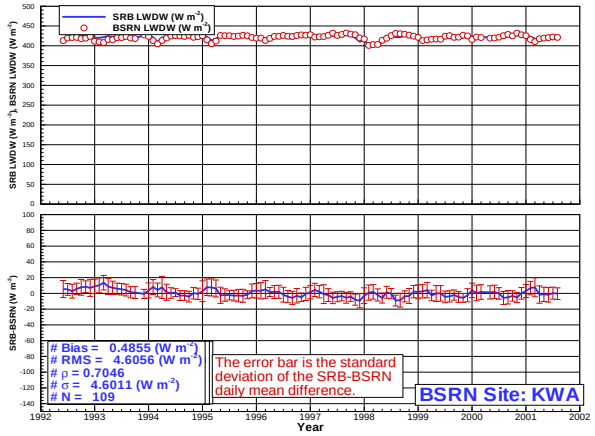

Figure 17: Time series of monthly means of SRB(V2.5) and BSRN longwave downward fluxes and difference thereof at BSRN site KWA (Kwajalein, Marshall Islands; 8.72°N, 167.73°E).

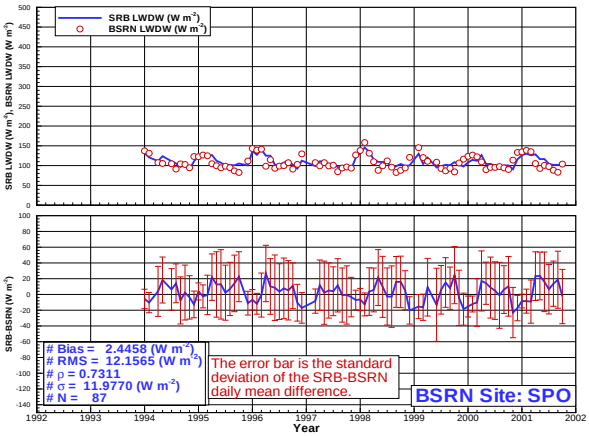

Figure 18: Time series of monthly means of SRB(V2.5) and BSRN longwave downward fluxes and difference thereof at BSRN site SPO (South Pole; 90.00°S, 0.00°E).

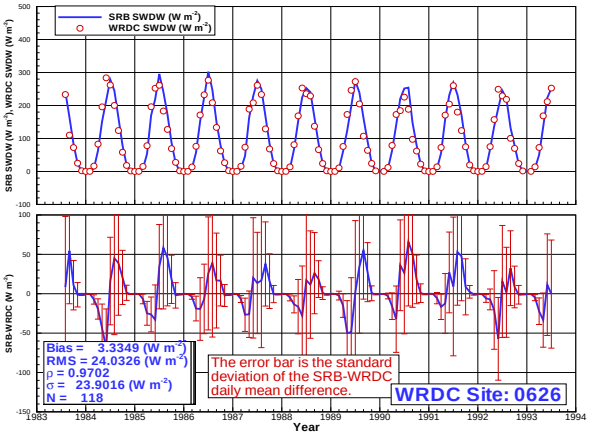

Figure 19: Time series of monthly means of SRB(V2.5) and WRDC shortwave downward fluxes and difference thereof at WRDC site 0626 (Wrangel Island, Russia; 70.58°N, 178.32°W).

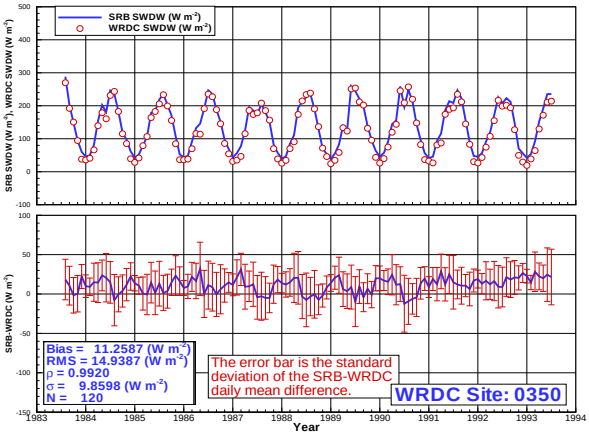

Figure 20: Time series of monthly means of SRB(V2.5) and WRDC shortwave downward fluxes and difference thereof at WRDC site 0350 (Klote, Switzerland; 47.29°N, 8.32°E).

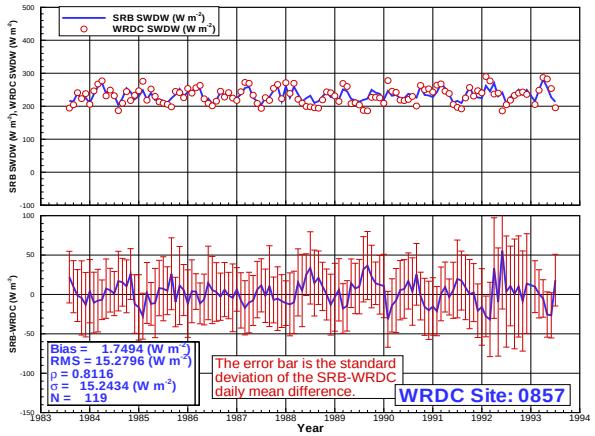

Figure 21: Time series of monthly means of SRB(V2.5) and WRDC shortwave downward fluxes and difference thereof at WRDC site 0857 (Narok, Kenya; 1.08°S, 35.50°E).

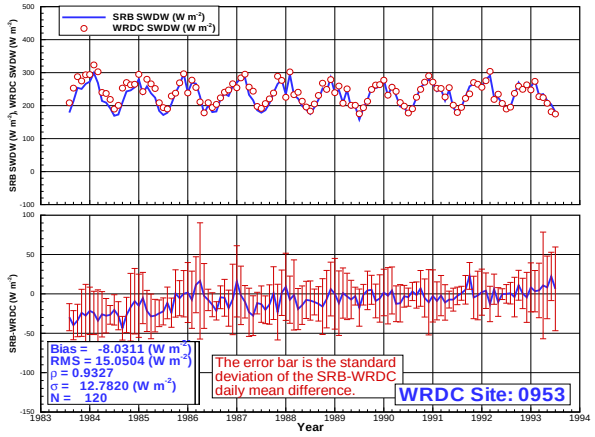

Figure 22: Time series of monthly means of SRB(V2.5) and WRDC shortwave downward fluxes and difference thereof at WRDC site 0953 (Bulawayo, Zimbabwe; 20.09°S, 28.37°E).

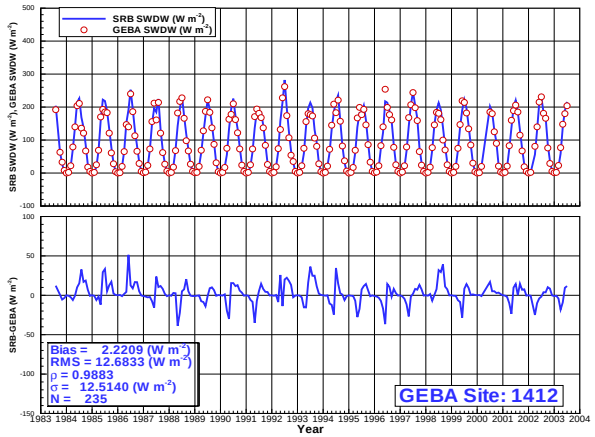

Figure 23: Time series of monthly means of SRB(V2.6) and GEBA shortwave downward fluxes and difference thereof at GEBA site 1412 (Kiruna, Sweden; 67.85°S, 20.23°E).

(Kiruna, Sweden), 1238 (Jokioinin, Finland), 1176 (Uccle, Belgium) and 1274 (Ajaccio, France) along with their SRB counterparts.

Altogether, 101 of the 797 GEBA sites have nearly continuous records during the period of two decades from 1983-2003.

The results presented in Figures 13-26 show the the SRB Version 2.5 and 2.6 data not only catch the magnitudes of the shortwave and longwave downward fluxes consistently with considerable accuracy, but the seasonality as well.

4 The Variability of the Data

Here we examine if there is any appreciable linear trend in the SRB data over the course of 21.5 years and how the data variability is associated with the El Niño Southern Oscillation (ENSO).

4.1 Linear Trend

In Figure 27, the *green* curve in the upper panel shows the sequence of the global mean of the SRB (Version 2.5) monthly means of shortwave downward fluxes at the Earth's surface, and the *red* curve shows the average of the SRB data at selected grids corresponding to 101 GEBA sites with continuous records. The purpose of the red curve is to see to what an extent the average of ground observations from these sites may represent the global average.

Interestingly, the seasonality of the SRB global mean is synchronous with that of the Southern Hemisphere, and the average from the selected grids shows a Northern Hemisphere seasonality which is much more pronounced than that of the global mean, apparently due to the fact that most of the 101 GEBA sites are in Northern Hemisphere.

The lower panel of Figure 27 shows the deseasonalized version of the upper panel. At the same time, the trends as derived from linear regression are shown in straight lines. Following the method of Weatherhead *et al.* (1998), autocorrelation of the data is considered. Computation of the partial autocorrelation coefficients indicates that only lag-1 autocorrelation is statistically significant, and consequently, an autoregressive model of order 1, it i.e., AR(1) model can be justifiably used to estimate the linear trend in the mean averaged both globally and at selected GEBA sites.

Thus the trends computed are $b_{SELECTED} = 0.0454$ ($\mathrm{W\,m^{-2}\,a^{-1}}$) and $b_{GLOBAL} = 0.0447$ ($\mathrm{W\,m^{-2}\,a^{-1}}$). Both the 95% confidence intervals

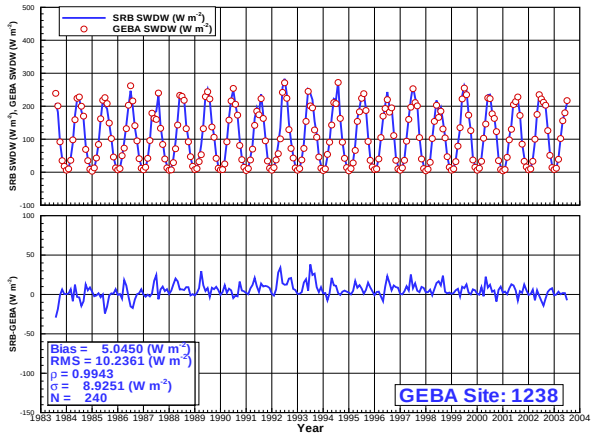

Figure 24: Time series of monthly means of SRB(V2.6) and GEBA shortwave downward fluxes and difference thereof at GEBA site 1238 (Jokioinen, Finland; 60.82°S, 23.50°E).

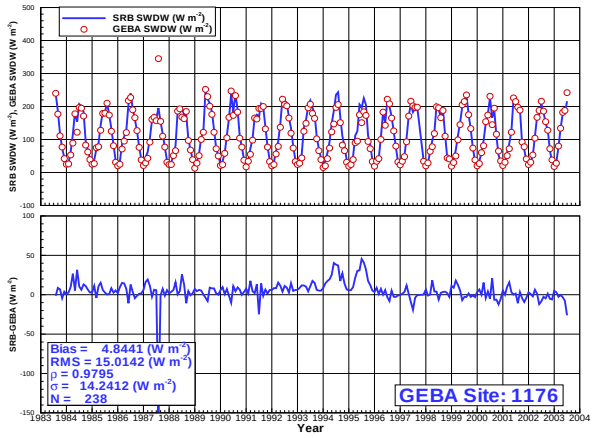

Figure 25: Time series of monthly means of SRB(V2.6) and GEBA shortwave downward fluxes and difference thereof at GEBA site 1176 (Uccle, Belgium; 50.80°S, 4.35°E).

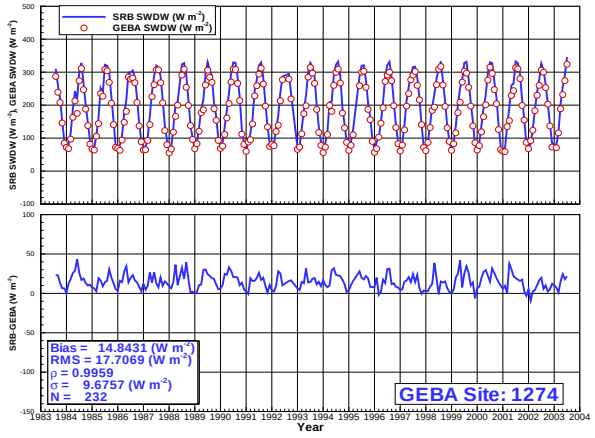

Figure 26: Time series of monthly means of SRB(V2.6) and GEBA shortwave downward fluxes and difference thereof at GEBA site 1274 (Ajaccio, France; 41.92°S, 8.80°E).

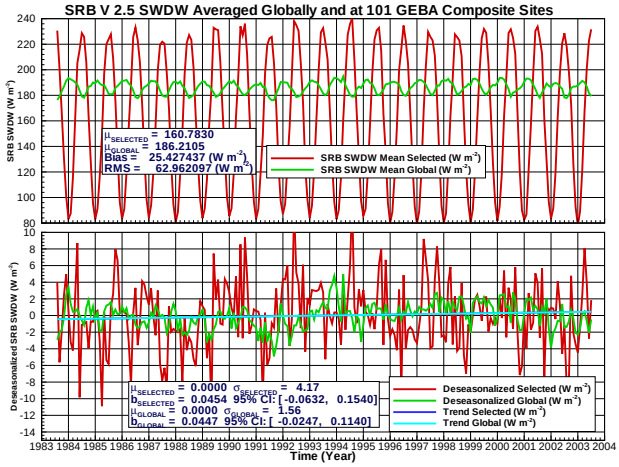

Figure 27: SRB(V2.5) shortwave monthly means averaged globally and at 101 GEBA composite sites. The upper panel shows the time sequences, and the lower panel shows the corresponding deseasonalized versions as well as the linear trends displayed in the data.

are wide due to the autocorrelation and stride 0, leaving small positive trends in uncertainty.

4.2 Correlation with the ENSO

To see the variablity of the SRB data, we computed the empirical orthogonal functions (EOFs) of the shortwave downward fluxes, and to emphasize the component associated with the ENSO, the range of interest is limited the Pacific region. The first EOF of the deseasonalized version of the data explain 20.60% of the total variance, and its coefficient is shown in Figure 28 along with the Southern Oscillation Index (SOI), and the correlation coefficient of the two curves is as high as 0.7083. Note that the boundary of the Pacific region is indicated in the figure.

As the figure indicates, there is a significant deterministic component of the shortwave downward flux that is associated with the ENSO. If a trend is to be computed for the reference of practical decision-makers, this process, along with other possible deterministic oscillatory processes should be identified and eliminated first.

5 Discussion and Conclusions

Despite the challenges involved in the GEWEX SRB project, the SRB Versions 2.5 and 2.6 algorithms generated the most comprehensive sur-

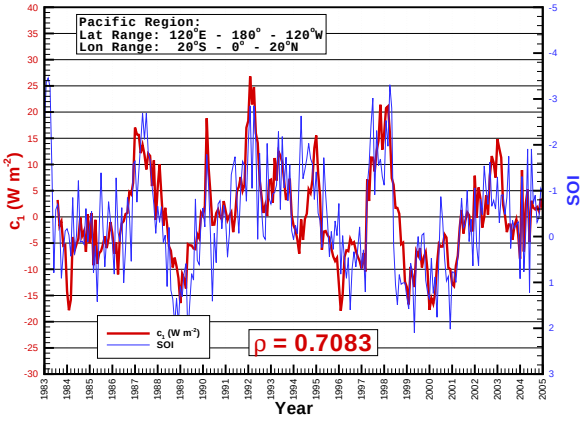

Figure 28: The coefficient of the first EOF of the SRB(V2.5) deseasonalized downward shortwave flux from July 1983 to December 2004 over the Pacific in comparison with the Southern Oscillation Index (SOI) over the same period. Note that the correlation coeffcient, ρ, is as high as 0.7083.

face radiation database from satellite-based observations. The improvement of Version 2.6 over Version 2.5 is that more accurate astronomical geometry of the sun is introduced. The time span of the database covers the time from July 1983 to December 2004, and the resolution is based on a nearly equal-area scheme of 44,016 grids which are $1^\circ \times 1^\circ$ around the Equator. The shortwave and longwave fluxes at the Earth's surface representing daily and monthly means turned out to be in very good agreement with the independently observed ground-based BSRN, WRDC and GEBA data. The SRB 3-hourly and 3-hourly-monthly data which are not shown in this study are equally in good agreement with their BSRN counterparts except they are, understandably, noisier than the daily and monthly means as manifested in their larger standard deviations.

In addition to the solar zenith angle, the cloudiness plays a significant role in the shortwave flux. The great temporal and spatial variablity of clouds manifests itself in the variablity of shortwave flux at the Earth's surface. However, the noise exhibited in the scatter and scatter density plots cannot be equally attributed to the SRB and ground-based data sets. As separate computation indicates, the ground-based time series contains slightly more variance than their SRB counterparts, which is due to the fact that each ground-based observation is conducted at a single point on the surface of the Earth that may experience the whole range of cloudiness from zero to the possible maximum while each of the SRB value represents an instant spatial average over a grid whose linear size ranges from about 111 to 192 Km. An SRB grid is thus less likely to experience the total cloud-free condition. So the time averaging process has removed, but not completely, the extra variance of the ground-based data as compared to their SRB counterparts.

Out of the ground-based sites, 8 BSRN sites, 55 WRDC sites and 101 GEBA sites have nearly continuous records over extended periods, and they are generally in good and consistent agreement with their SRB counterparts. In the case of SRB-BSRN comparisons, the agreement tends to be better in lower latitudes than higher ones. Although we tend to treat the ground-based observations as the "truth", we need to be careful in evaluating the quality of satellite-ground agreement. There may be errors attributable to technical aspects of the instruments, the micro-environments around the instruments, and human errors as well.

Compared with the shortwave fluxes, the longwave fluxes behave more predictably, exhibiting much less irregularity, and the scatter and scatter density plots show few points that can be considered as *outliers*. This can be attributed to the fact that the longwave radiation intensity is determined by the temperature profile of the atmosphere and other components residing therein, and the temperature is not as prone to change as the solar radiation transferring in the atmosphere. As a consequence, both the bias and RMS errors in the longwave comparisons are markedly smaller than their shortwave counterparts.

The trend estimate on the global and regional scales is interesting and a challenge both mathematically and for practical decision-makers. Based on an AR(1) model, the global mean of the SRB Version 2.5 does not show an appreciable linear trend over the years from July 1983 to June 2003.

The first EOF coefficient of the deseasonalized global mean of monthly means of the SRB Version 2.5 shortwave downward flux over the Pacific region explains a significant part of the total variance and is highly correlated with the ENSO. This means that climatic variations associated with the ENSO leave unmistakable signals in the time sequence of the global radiation field.

REFERENCES

Gupta, S.K., N.A. Ritchey, A.C. Wilber, C.H. Whitlock, G.G. Gibson and P.W. Stackhouse Jr.,

1999: A Climatology of Surface Radiation Budget Derived from Satellite Data. *Journal of Climate*, **12**, 2691-2710.

McArthur, L.J.B., 1998: Baseline Surface Radiation Network (BSRN) Operational Manual. WMO/TD-No. 879.

Ohmura, A. *et al.*, 1998: Baseline Surface Radiation Network (BSRN/WCRP): New Precision Radiometry for Climate Research. *Bulletin of the American Meteorological Society*, **79**(10), 2115-2136.

Philipona, R. *et al.*, 1998: The Baseline Surface Radiation Network Pyrgeometer Round-Robin Calibration Experiment. *Journal of Atmospheric and Oceanic Technology*, **15**, 687-696.

Pinker, R.T., J.D. Tarpley, I. Laszlo, K.E. Mitchell, P.R. Houser, E.F. Wood, J.C. Schaake, A. Robock, D. Lohmann, B.A. Cosgrove, J. Sheffield, Q.Y. Duan, L.F. Luo, R.W. Higgins, 2003: Surface radiation budgets in support of the GEWEX Continental-Scale International Project (GCIP) and the GEWEX Americas Prediction Project (GAPP), including the North American Land Data Assimilation System (NLDAS) Project. *Journal OF Geophysical Research-Atmospheres*, **108**, D22, 8844.

Pinker, R.T., B. Zhang, E.G. Dutton, 2005: Do Satellites Detect Trends in Surface Solar Radiation? *Science*, **308**, 850-854.

Randall, D., S Krueger, C Bretherton, J Curry, P Duynkerke, M Moncrieff, B Ryan, D Starr, M Miller, W Rossow, G Tselioudis, B Wielicki, 2003: Confronting models with data - The GEWEX cloud systems study. *Bulletin OF THE American Meteorological Society*, **84**, 455-469.

Suarez, M.J. (ed.), 2005. Documentation and Validation of the Goddard Earth Observing System (GEOS) Data Assimilation System-Version 4. *Technical Report Series on Global Modeling and Data Assimilation*, Vol. **26**. April, 2005.

Weatherhead, E.C. *et al.*, 1998. Factors Affecting the Detection of Trends: Statistical Considerations and Applications to Environmental Data. *Journal of Geophysical Research*, **103**(D14), 17,149-17,161.

Wild, M., *et al.*, 2005: From Dimming to Brightening: Decadal Changes in Solar Radiation at Earth's Surface. *Science*, **308**, 847-854.

Zhang, T., P.W. Stackhouse, Jr., S.J. Cox, G.L. Smith and M. Chiacchio, 2003: Analysis of the Surface Radiation Budget Data in Terms of Empirical Orthogonal Functions (EOFs). *Fall Meeting of the American Geophysical Union*. December 8 - 12, 2003. San Francisco.

Zhang, T., P.W. Stackhouse Jr., S.K. Gupta, S.J. Cox and J.C. Mikovitz, 2004: Signals of Climate Variations in the WCRP/GEWEX SRB Datasets and Their Connections with Other Climate Indices. *Proceedings of the International Radiation Symposium 2004 (IRS 2004)*, Busan, Korea, August 23-28, 2004.